Stabilization of apo α-lactalbumin by binding of epi-gallocatechin-3-gallate: experimental and molecular dynamics study

Milica Radibratovic[a], Ayah al-Hanish[b], Simeon Minic[b], Mirjana Radomirovic[b], Milos Milcic[c], Dragana Stanic-Vucinic[b], and Tanja Cirkovic Velickovic[b,d,e,#]

[a]Center for Chemistry - Institute of Chemistry, Technology and Metallurgy, University of Belgrade, Belgrade, Serbia

[b]Center of Excellence for Molecular Food Sciences & Department of Biochemistry, University of Belgrade - Faculty of Chemistry, Belgrade, Serbia

[c]Center for Computational Chemistry and Bioinformatics & Department of Inorganic Chemistry, University of Belgrade - Faculty of Chemistry, Belgrade, Serbia

[d]Ghent University Global Campus, Yeonsu-gu, Incheon, South Korea

[e]Faculty of Bioscience Engineering, Ghent University, Ghent, Belgium

#Correspondence:

Prof. dr Tanja Cirkovic Velickovic

Ghent University Global Campus, Yeonsu-gu, Incheon, South Korea

E-mail address: Tanja.Velickovic@ghent.ac.kr

Abstract

α-Lactalbumin (ALA) is a Ca2+-binding protein which constitutes up to 20% of whey protein. At acidic pH, and in the apo-state at elevated temperatures, ALA is the classic 'molten globule' (MG). This study examined epigallo-catechin-3-gallate (EGCG) binding to ALA in its apo form (apoALA) and stabilizing effect on protein structure thereof.

EGCG binds to apoALA in both native and MG state. The complex of EGCG and ALA is more stable to thermal denaturation. The docking analysis and molecular dynamic simulation (MDS) showed that Ca2+ removal decreased conformational stability of ALA, because of the local destabilization of Ca2+-binding region. EGCG binding to apoALA increases its stability by reverting of conformation and stability of Ca2+-binding region. Therefore, EGCG-induced thermal stability of apoALA is based on increased apoALA conformational rigidity. This study implies that during gastric digestion of tea with milk EGCG would remain bound to ALA, albeit in the Ca2+-free form.

Key words: apo α-lactalbumin, epigallocatechin-3-gallate, noncovalent interactions, protein stability, fluorescence quenching, molecular dynamics simulation

1. Introduction

α-Lactalbumin (ALA) is a small (Mr 14 200), acidic (pI 4-5), Ca2+-binding protein that constitutes up to 20% of whey protein (Permyakov & Berliner, 2000). Because of clean flavour profile, good water solubility and very low aggregation upon heating, it can be used as supplement protein to diverse food products and beverages. In addition, due to high content of essential amino acids, including tryptophan, lysine and branched-chain amino acids, it has potential as a nutritional supplement for neurological function and a component of infant formulas (Layman, Lonnerdal, & Fernstrom, 2018).

Structurally homologous to the lysozyme family, native ALA consists of two domains: a large α-helical domain and a small β-sheet domain. ALA possesses a single strong Ca2+-binding site, and for this reason it is frequently used as a simple, model Ca2+-binding protein (Permyakov & Berliner, 2000). The high-affinity Ca2+-binding site is located at the junction of the subdomains, where Ca2+ ion is coordinated by Asp82, Asp87, Asp88, Lys79, Asp84, and two water molecules. ALA has several partially folded intermediate states. It is very attractive for studies of the properties and structure of intermediate molten globule-like states, since at acidic pH, and in the apo-state at elevated temperatures, ALA is the classic 'molten globule' (MG) (Permyakov & Berliner, 2000). In MG state, a protein has preserved most of the secondary structure features, but its tertiary structure is fluctuating (Veprintsev, Permyakov, Permyakov, Rogov, Cawthern, & Berliner, 1997).

Green tea, a polyphenol rich source, is one of the most-consumed beverage in the world. Catechins represent up to 85% of the total tea polyphenols, with (−)-epigallo-catechin 3-gallate (EGCG) is known as the most abundant (up to 50%) (Ferruzzi, 2010). The most of health-promoting effects of the tea have been attributed to EGCG and many studies have been done to show the health benefits provided by foods containing EGCG. In addition, EGCG has been studied for its potential as natural antioxidant and antimicrobial agent for preservation of the food quality and enhancing the food safety (Nikoo, Regenstein, & Gavlighi, 2018). Poor EGCG bioavailability and stability in specific food matrices can be improved by its encapsulation with food proteins. Milk proteins, are excellent carriers for encapsulation of EGCG, improving its stability and protecting its activity during prolonged storage (Shi, Shi, Li, Yang, Cai, Li, et al., 2018). In order to produce functional dairy foods, milk, yoghurt and cheese can be enriched with

green tea catechins (Amirdivani & Baba, 2015; Najgebauer-Lejko, Sady, Grega, & Walczycka, 2011; Rashidinejad, Birch, & Everett, 2016; Rashidinejad, Birch, Sun-Waterhouse, & Everett, 2014)

Interactions of α-lactalbumin were investigated with phenolic acids commonly found in food (Zhang, Yu, Sun, Guo, Ding, Liu, et al., 2014), procyanidins (Prigent, Voragen, van Koningsveld, Baron, Renard, & Gruppen, 2009), genistein, kaempferol (Mohammadi & Moeeni, 2015a), resveratrol (Hemar, Gerbeaud, Oliver, & Augustin, 2011) and curcumin (Mohammadi & Moeeni, 2015b). Binding of anthocyanin extract from grapes by whey protein isolate presumbly involves ALA as a tight binder of malvidine 3-glucoside (Stanciuc, Turturica, Oancea, Barbu, Ionita, Aprodu, et al., 2017). It has been shown that major green tea catechin EGCG binds covalently (Wang, Zhang, Lei, Liang, Yuan, & Gao, 2014) and also forms stable non-covalent complexes with ALA (Al-Hanish, Stanic-Vucinic, Mihailovic, Prodic, Minic, Stojadinovic, et al., 2016).

In silico analysis suggests that ALA contains at least one putative high-affinity EGCG-binding site, which is positioned in the hydrophobic pocket between two domains and interacts with the residues of aromatic cluster II, including dominant fluorophore Trp104 (Al-Hanish, et al., 2016). In the only two reported molecular docking studies of binding of polyphenol compounds to ALA Mohammadi et al. (Mohammadi & Moeeni, 2015a, 2015b) have demonstrated that resveratrol, curcumin, genistein and kaempferol bind to quite different regions on ALA.

ALA in its apo-form has ability to interact with hydrophobic substances such as vitamin D3 (Delavari, Saboury, Atri, Ghasemi, Bigdeli, Khammari, et al., 2015), hydrophobic peptides like the bee venom melittin (Permyakov, Grishchenko, Kalinichenko, Orlov, Kuwajima, & Sugai, 1991), model lipid membranes (Chaudhuri & Chattopadhyay, 2014), fatty acids (Barbana, Perez, Sanchez, Dalgalarrondo, Chobert, & Haertle, 2006). The bioactive complex between ALA and oleic acid is known as BAMLET/HAMLET/GAMLET (Bovine/Human/Goat ALA made lethal to tumours), and it has been shown to be cytotoxic to a range of cancer cell lines (Mok, Pettersson, Orrenius, & Svanborg, 2007). The ALA portion of HAMLET/BAMLET is in a MG-like conformation under physiological conditions of gastric environment and it is considered that in acidic pH it binds oleic acids into an active complex.

Although these data suggest that EGCG may interact with 124 apo form of ALA, up to date, there are no studies describing interactions of polyphenols, including EGCG, and ALA in its

calcium depleted form, nor there are studies on the stabilizing effect of polyphenol on metal-binding proteins in their apo form in general.

The aim of our study was to examine if green tea polyphenol binds to the apo form of ALA in neutral and acidic conditions. Moreover we examined if the polyphenol binding can stabilize native and MG protein structure and how the binding influences the calcium-binding site in particular. The experimental investigations were supported by docking analysis and molecular dynamics of apo and holo-ALA complexes with EGCG.

2. Material and methods

2.1. Isolation of holoALA and preparation of apoALA

HoloALA was purified from raw bovine milk and separated from β-lactoglobulin (BLG) by a combination of gel filtration and ion-exchange chromatography, as described previously (Al-Hanish, et al., 2016). Protein was subject to Ca^{2+}-depletion by extensive dialysis in the presence of EDTA (50 mM sodium phosphate buffer pH 7.2) in order to prepare apo-ALA. EGCG, glycine, EDTA, $CaCl_2$ and sodium dihydrogen phosphate were purchased from Sigma Aldrich (St. Louis, MO, USA). Deionized water used in the experiments was purified by a Milli-Q system (Millipore, Molsheim, France).

2.2. Fluorescence spectroscopy measurements

All fluorescence spectra were recorded on FluoroMax®-4 spectro-fluorometer (HORIBA Scientifc, Japan) under thermostated conditions, while the excitation and emission slit widths were set to 5 nm.

2.2.1 Quantification of EGCG binding to apo- and holo-ALA

Binding of EGCG to ALA was studied by the fluorescence quenching approach using the intrinsic fluorescence of ALA as a probe. The steady-state fluorescence spectra were measured at 6 and 37 ^{o}C, while the following buffers were used: 0.1 M HCl (containing 34 mM NaCl) pH 1.2, 0.1 M glycine-HCl pH 2.5 and 50 mM phosphate buffer pH 7.2. All buffers contained 1 mM

EDTA. Protein concentration was constant (1 µM), while the EGCG concentrations varied from 0 to 20 µM. The excitation wavelength was set at 280 nm and the emission spectra were read from 290 to 450 nm. The appropriate blanks corresponding to the various EGCG concentrations (free EGCG in buffer) were subtracted to correct background of fluorescence.

Instead of using double logarithmic Stern-Volmer equation, where added ligand concentration is approximated as the free ligand concentration ($L_{free} \approx L_{added}$), for estimation of the association constant (Ka) for EGCG binding to ALA more accurately, equation:

$$\log\frac{F_0 - F}{F} = -n\log\frac{1}{[EGCG] - [ALA]\frac{F_0 - F}{F_0}} + n\log K_a$$

was used (Bi, Ding, Tian, Song, Zhou, Liu, et al., 2004), where fraction of ligand bound to protein was taken into account. [ALA] and [EGCG] are total concentration of protein (apoALA or holoALA) and EGCG, respectively, and Ka is the binding constant. F_0 and F (at 335 for the measurements at pH 7.2 and at 345 nm for the measurements at pH 2.5 and 1.2) represent fluorescence of protein in the absence and in the presence of ligand, respectively.All binding experiments were performed in the presence of EDTA to prevent changes in the fluorescence intensity due to trace amounts of ions present in buffers and EGCG solution. Determination of binding constants of EGCG to holo-ALA was the same as described above, except that buffers contained 1 mM Ca^{2+}, instead of 1 mM EDTA.

2.2.2. *Determination of melting point of apo- and holo-ALA*

Thermal denaturation of 2.5 µM apoALA in presence and absence of 50 µM EGCG was performed in 50 mM sodium phosphate buffer pH 7.2, containing 1 mM EDTA, at the temperature range 10–60 ^{o}C, with temperature increasing rate 0.6 ^{o}C/min. Fluorescence spectra were measured between 315 and 365 nm with excitation at 280 nm. Spectra of free EGCG (50 µM) and buffer were subtracted from spectra of apoALA-EGCG complex free apo-ALA, respectively. Obtained spectra were smoothed using adjacent-averaging method with 10 points of window in OriginPro 8 software. The results were expressed as dependence of the emission maximum on temperature. Obtained curves were fitted with a sigmoidal function. The inflection point in the plot was taken as melting temperature (T_m) of apoALA. The melting temperature was also determined after the first derivative analysis of the emission maximum dependence on

temperature. The procedure for holoALA melting was the same as described above, except that denaturation was performed in the presence of 1 mM Ca^{2+}, instead of 1 mM EDTA, while the temperature range was set to 30-75 ^{o}C.

2.3. Circular dichroism and secondary structure calculation

CD spectra of ALA in the absence and presence of EGCG were recorded on a JASCO J-815 spectropolarimeter (JASCO, Japan) under thermostated conditions (20 °C). Spectra were recorded in 0.1 nm steps at a rate of 50 nm/min. Far UV CD spectra were recorded in 185-260 nm wavelength range a 0.01 cm path length quartz cell, and near UV spectra were recorded in 260-320 nm range using 1 cm length cell. Obtained spectra were the averages of three accumulated scans with subtraction of the baseline. The reported spectra are the average of at least two experimental results obtained independently. Percentage of secondary structure motifs was calculated from the CD spectra using the CONTIN algorithm available in the CDPro software package by referencing to SP29 protein set (29 soluble proteins with known secondary structures).

Protein concentration was 70 μmol L^{-1} (1 mg ml^{-1}), while EGCG concentration was 140 μmol L^{-1}. Samples were prepared in 50 mmol L^{-1} sodium phosphate pH 7.2., 100 mM glycine buffer pH 2.5 and 100 mM HCl (containing 34 mM NaCl), pH 1.2.

Induced CD spectra for apoALA-EGCG samples were obtained using equation:

induced $CD_{ALA-EGCG} = CD_{ALA-EGCG} - (CD_{ALA} + CD_{EGCG})$,

where $CD_{ALA-EGCG}$ is the spectra of the apoALA−EGCG sample, while CD_{ALA} and CD_{EGCG} represent the spectra of samples containing only apoALA and EGCG, respectively.

2.4.Computational details

In order to compare stability of apoALA and holoALA the same initial crystal structure was used (holoALA, PDB ID: 1F6S). The apoALA structure was obtained by removing of Ca^{2+} ion from the crystal structure. The protonation state of each titratable amino acid was estimated using the H++ program (Anandakrishnan, Aguilar, & Onufriev, 2012). All MD simulations were performed with the NAMD 2.9 program using CHARMM27 force field (Mackerell, Feig, & Brooks, 2004; Phillips, Braun, Wang, Gumbart, Tajkhorshid, Villa, et al., 2005). Starting structures were solvated in a box of TIP3P water, followed by neutralization and addition of

NaCl (total concentration was 150 mM). The obtained system was minimized to remove possible close contacts between atoms, followed by 250 ps of equilibration in NVE ensemble. Next, the system was set to 40 ns production run in NPT dynamics using the Langevin piston pressure control at 310 K and 1.01325 bars. Periodic boundary conditions and the Particle-mesh Ewald method were implemented for a complete electrostatic calculation. The trajectory was analyzed with the VMD (version 1.9.2) (Humphrey, Dalke, & Schulten, 1996) and MDTRA program (Popov, Vorobjev, & Zharkov, 2012). After removing Ca^{2+} ion from the crystal structure MDS was set to 20ns in order to provide a relaxed apoALA structure followed by molecular docking experiment using AutoDock Vina program (version 1.1.2) (Trott & Olson, 2009). The ligand was prepared as described in Al Hanish et al. (Al-Hanish, et al., 2016). All trajectories were clustered using UCSF Chimera program (Pettersen, Goddard, Huang, Couch, Greenblatt, Meng, et al., 2004). For each trajectory the average structure from the most numerous cluster was obtained and further analyzed. In order to trace displacement of amino acids that constitute Ca^{2+} binding site in MDS trajectory of apoALA and apoALA/EGCG systems, Ca^{2+} ion was added by aligning those structures with holoALA structure.

2.5. Statistics

All results were obtained at least in duplicate and results were shown as mean ± standard deviation. For comparison of EGCG binding constants to apo- and holo-ALA at different temperatures and pHs, as well as for evaluation of effects of EGCG binding on protein secondary structures content, an analysis of variance (ANOVA) of data was performed and means comparisons were done using Turkey test. In all statistical analyses, differences were considered significant in the case $p<0.05$.

3. Results and discussion

3.1 EGCG forms a non-covalent complex with apoALA

ALA is intrinsically fluorescent due to the presence of four tryptophans (Trp-118, Trp-60, Trp-104 and Trp-26) resulting in emission maximum at 329 nm in its native form (Permyakov,

Permyakov, Deikus, Morozova-Roche, Grishchenko, Kalinichenko, et al., 2003). In ALA partially unfolded form of molten globule emission maximum is about 340 nm, while for fully unfolded state it is 351 nm (Chakraborty, Ittah, Bai, Luo, Haas, & Peng, 2001). As the tea is frequently consumed with the addition of milk, EGCG bioavailability from tea is mostly determined by interactions of EGCG with milk proteins. Therefore, we examined binding of EGCG to ALA at physiological conditions of gastrointestinal tract: at pH 7.2 (pH of saliva and intestine) and pH 1.2 and 2.5 (gastic pH range during digestion) at 37 ºC. We also investigated EGCG binding at low temperature, 6 ºC, at all three pH values for comparison, having in mind apoALA thermal instability.

In absence of EGCG, emission maximum at about 330 nm can be observed only at pH 7.2, in holoALA at 6 ^{o}C and 37 ^{o}C, and apoALA at 6 ^{o}C, suggesting preserved native structure of both forms (Table 1, Figure S1). However, in apoALA at pH 7.2 and 37 ^{o}C maximum increased to 341 nm due to apoALA thermal instability and partial disruption of its tertiary structure most probably resulting in MG. At pH 2.5 and pH 1.2, at 6 ^{o}C, both ALA forms have partially disturbed tertiary structure to MG-like, reflecting in emission maxima at about 344-345 nm. This is consequence of protonation of five Asp residues in Ca^{2+}-binding region resulting in the loss of Ca^{2+} in holoALA and charge repulsion of Asp carboxylates in both forms. In acidic environment (pH 2.5 and pH 2.5) at 37 ^{o}C, further slight red shift to about 346-347 nm point to more pronounced unfolding.

With the addition of increasing concentrations of EGCG, the fluorescence intensity of holoALA and apoALA decreases in neutral and acidic conditions, and at both temperatures. Absence of noticeable shift in emission maxima indicates that EGCG binding does not disturb significantly tertiary structure of both ALA forms, even at EGCG/protein ratio 20:1. Tryptophan fluorescence spectrum of the apoALA at pH 7.2 and at cold temperature is dominated by emission from Trp104, (Chakraborty, Ittah, Bai, Luo, Haas, & Peng, 2001) situated in the cleft region separating the α-helical and β-sheet lobes (Malinovskii, Tian, Grobler, & Brew, 1996. Therefore, EGCG most probably binds to the cleft region of the apoALA, similarly to its binding to holo-form (Al-Hanish, et al., 2016).

The obtained binding constants (Ka) of apoALA and holoALA are of similar magnitude at all three tested pH values and in two different temperatures (Table 1), with tendency of both forms to have lower Ka at 37 ^{o}C and at very acidic conditions (pH 1.2). Indeed, for apoALA,

statistically lower Ka was obtained in pH 1.2 at 37 ºC, where apoALA is in less ordered state, than in pH 7.2 at 6ºC, where apoALA is in its native conformation. Similarly, for holoALA, EGCG shows statistically higher Ka in pH 7.2 at 37C, where holo form is native, than at acidic conditions (pH 2.5 and 1.2) at 37 ºC, where holo form looses Ca^{2+} and consequently have less ordered MG-like structure due to thermal instability at 37 C (Table 1). Similar magnitude of EGCG binding to both ALA forms at all tested conditions, even in very acidic conditions and at 37ºC, is due to at least partially preserved ALA structure e.g. native and MG/MG-like structure. Actually, at all tested conditions emission maxima do not reach 351 nm, characteristic for unfolded protein, implying that Trp residues are still partially buried in nonpolar environment and that protein structure is not unfolded. Obtained binding parameters for apoALA and EGCG are similar to those obtained for complexes of EGCG and other proteins (Al-Hanish, et al., 2016; Perusko, Al-Hanish, Mihailovic, Minic, Trifunovic, Prodic, et al., 2017; Vesic, Stambolic, Apostolovic, Milcic, Stanic-Vucinic, & Cirkovic Velickovic, 2015) (Table 1). These results suggests that, although EGCG has lower affinity for ALA forms with less ordered structure, such as MG-like, it remains binds bound to apoALA in gastrointestinal tract e.g. at acicdic pH and, 37 ºC.

Table 1. Binding constants of EGCG to apoALA and holoALA, and their emission maxima (excitation at 280 nm) at two different temperatures and three different pH. The results were obtained in triplicate and different small superscripts (a–d) denote significant differences ($p < 0.05$).

apoALA				
pH	6 C		37 C	
	Em max (nm)	EGCG binding constants (x104 M-1)	Em max (nm)	EGCG binding constants (x104 M-1)
1.2	344	1.63±0.30 ^{abc}	346	0.75±0.15 ^{b}
2.5	344	1.60±0.23 ^{abc}	347	1.61±0.51 ^{abc}
7.2	330	2.18±0.26 ^{ac}	341	1.80±0.39 ^{abc}
holoALA				

pH	6 C		37 C	
	Em max (nm)	EGCG binding constants (x104 M-1)	Em max (nm)	EGCG binding constants (x104 M-1)
1.2	345	1.31±0.28 [bc]	345	0.76±0.07 [bd]
2.5	344	1.22±0.10 [bc]	346	1.28±0.12 [bc]
7.2	328	1.95±0.12 [acd]	329	2.59±0.78 [a]

3.2. EGCG binds to apoALA in native and MG state inducing slight structure changes

The effect of formation of apoALA/EGCG complexes on the structure of apoALA was studied by far-UV and near-UV CD spectroscopy at 20 C. At pH 7.2 holo and apo form of ALA demonstrate similar far UV spectra (Fig S2A). Similar intensity of CD signal in near UV region (Fig S2B) demonstrate that apoALA has native tertiary structure.

In acidic conditions, according to far UV CD spectrum secondary structure was slightly changed where decrease in $[\theta]_{222/208}$ points to slightly disturbed noncovalent hydrophobic interactions between helices (Figs. S3A and S4A). However, in acidic environment both ALA forms have drastically disturbed tertiary structure, as reflecting in complete loss of signal in near UV CD spectrum (Figs. S32B and S4B). This demonstrates that at acidic conditions both apoALA and holoALA have typical molten globule conformation, retaining a substantial amount of secondary structure, but lacking the fixed packing interactions of the native state conformation.

In far UV CD spectra the interaction between EGCG and apoALA at ratio 2:1 caused a slight change at all three pH values, indicating that the EGCG induced slight alteration of the protein secondary structure (Figure 1A-C). At neutral, as well as acidic conditions in apoALA-EGCG complex there is tendency of decrease in α-helix content in favour of β-structures (Table S1), similarly to holoALA and EGCG complex (Al-Hanish, et al., 2016).

EGCG binding induced CD signal in the near UV region at all tested pH, with positive amplitudes centring at 275 nm (Figure 1D). These results further support EGCG binding at all three pH values, e.g. to native apoALA and its molten globule conformation. Slightly higher induced CD signal at acidic conditions suggests that EGCG binding induce more pronounced changes in tertiary structure when apoALA is in its less ordered state.

The results of CD spectroscopy imply that EGCG binds to apoALA whether it is in its native or molten globule conformation, inducing slight change in secondary, as well as in tertiary structure. According to obtained results, during gastic digestion of consumed tea with milk EGCG remains bound to ALA regardless if it is in apo form and molten globule conformation. Similarly, during gastric digestion of supplements/food fortified with EGCG encapsulated in ALA-based carriers, EGCG would be still bound to ALA. Moreover, it can be expected that other low molecular mass food-derived ligands bound to holoALA in food matrix remain bound to apoALA after Ca2+ loss in gastric compartment.

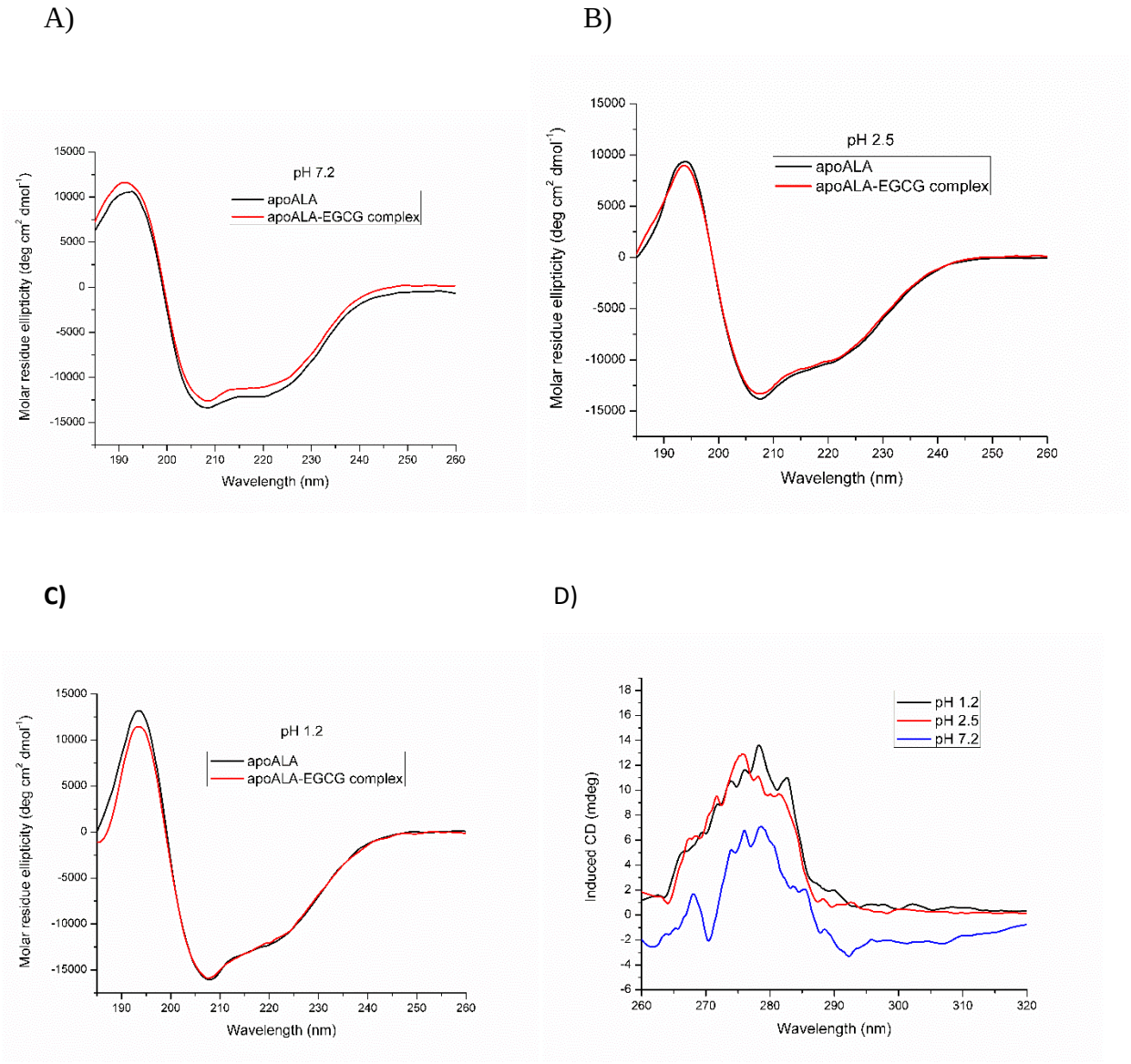

Figure 1. Far UV CD spectra of apoALA in the presence of EGCG (1:2) in 50 mM phosphate

buffer pH 7.2 (A), 100 mM glycine buffer pH 2.5 (B) and 100 mM HCl (containing 34 mM NaCl), pH 1.2 (C). D) Induced CD spectra of apoALA in the presence of EGCG (1:2) in near UV range.

3.3. Docking analysis of EGCG binding to apoALA

EGCG docked to apoALA at neutral pH interacts with similar set of residues as with holoALA (Figs. 2A and 2B), being positioned also at the cleft between α-helical and β-sheet subdomains.

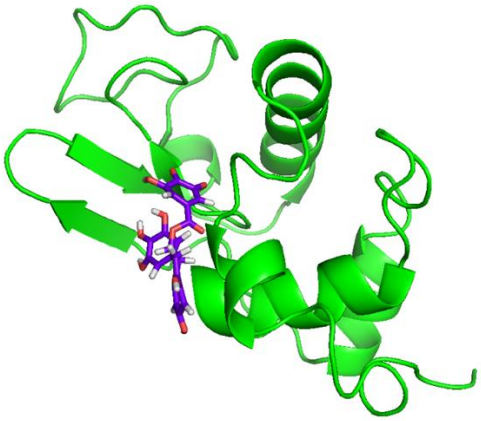

	apoALA-EGCG*	apoALA-EGCG Cl. 1	apoALA-EGCG Cl. 2	apoALA-EGCG Cl. 3	holoALA-EGCG*	holoALA-EGCG Cl. 1	holoALA-EGCG Cl. 2	holoALA-EGCG Cl. 3	holoALVit D*
His32			•	•	•				•
Thr33			•	•	•				•
Val42				•					
Asn44				•	•				•
Glu49	•	•	•	•	•	•	•	•	•
Phe 53	•			•	•	•	•	•	
Gln54	•	•		•	•	•	•	•	•
Asn56	•							•	•
Lys58									•
Asn102						•	•	•	
Tyr103	•	•		•	•	•		•	•
Trp104	•		•	•	•	•	•	•	•
Leu105	•	•	•	•	•				•
Ala106	•	•	•	•	•				•
Ala109	•			•					•
Leu110		•	•	•					•

Figure 2. A) The molecular docking analysis reveals the high-affinity site for binding EGCG to apoALA (PDB ID 1F6S with removed Ca^{2+} ion). Color codes: carbon-violet, oxygen-red, hydrogen-white, nitrogen-blue. **B**) EGCG-interacting residues in apoALA and holoALA found by docking (*), and in representative structures of the main three clusters of apoALA and holoALA after MDS. Interactions of vitamin D docked to holoALA are shown for comparison (Delavari, et al., 2015). EGCG-interacting residues of hydrophobic box are shaded in yellow (aromatic cluster I) and green (aromatic cluster II). ApoALA structure was obtained by Ca^{2+} removal from crystal structure of holoALA (PDB ID 1F6S). For both holoALA-EGCG and apoALA-EGCG, all conformations during 40 ns MDS were clustered, and the most representative structure for three main clusters are inspected for existence of interactions with EGCG.

3.4 Protein stability in a complex with EGCG

It is known that depletion of ALA from Ca^{2+} leads to a significant drop in protein's stability to thermal denaturation (Permyakov & Berliner, 2000; Sugai & Ikeguchi, 1994) and the melting

points of holo and apo forms of the protein may differ up to around 40 ^{o}C (Veprintsev, Permyakov, Permyakov, Rogov, Cawthern, & Berliner, 1997). In the absence of calcium ions, but in the presence of physiological concentrations of magnesium, sodium and potassium ions, the thermal transition of apoALA occurs in the region from about 30 to 45°C (Permyakov & Berliner, 2000).

We have used a method of intrinsic Trp fluorescence increase during the denaturation of protein to monitor denaturation transition point of apoALA and its complex with EGCG at pH 7.2. Denaturation of ALA leads toward red shift of protein emission peak, giving opportunity for studying its thermal unfolding. The melting point (Tm) that we determined by this method is in agreement with previously published studies (Veprintsev, Permyakov, Permyakov, Rogov, Cawthern, & Berliner, 1997). Tm values obtained by sigmoidal fit of melting curves demonstrated a difference of 22 ^{o}C in melting points of apo and holo ALA (Fig. 3). By this method we found that, compared to free apoALA (Tm = 28.3 C), apoALA-EGCG complex has greater thermal stability (Tm = 32.0 C). The stabilizing effect on the structure of apoALA (increase in Tm of 3.7 C) in more pronounced than on the structure of holo-form (increase in Tm of 0.8 C) of the protein (Figure 3). Tm values obtained by the first derivative of melting curves are similar as those obtained by sigmoidal fit (Fig. S5), Tm of apoALA and apoALA-EGCG are 28.1 C and 31.6 C, respectively (3.5 C difference), while Tm of holoALA and holoALA-EGCG are 48.0 C and 50.6 C (2.6 C difference).

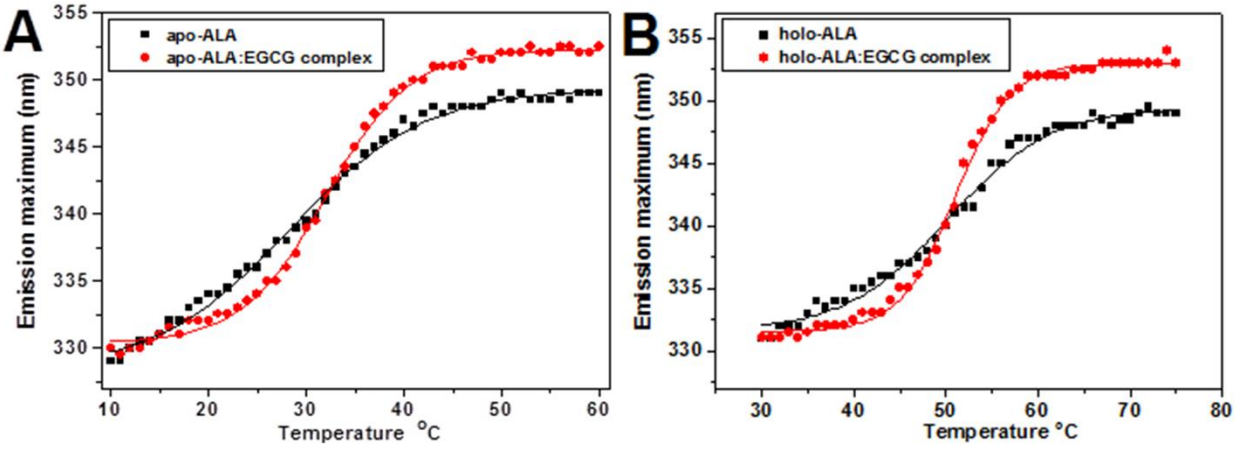

Figure 3. Temperature dependence of 2.5 µM apoALA (A) and holoALA (B) fluorescence maxima (excitation at 280 nm) in the absence and the presence of 50 µM EGCG in 50 mM phosphate buffer pH 7.2

3.5. Molecular dynamics simulation (MDS) of apoALA in complex with EGCG

To investigate the origin of increased conformational stability of apoALA in complex with EGCG, MDS study was undertaken for holoALA, apoALA, holoALA/EGCG complex and apoALA/EGCG complex. EGCG-apoALA interactions found by docking are found in all three MDS clusters, suggesting that docked EGCG remains bound in the same binding site during simulation. Residues are found to interact with EGCG docked to holoALA, indicating that EGCG is bound to both ALA forms at the same binding site. Beside, several additional interactions are found in apoALA-EGCG clusters (with His32, Thr33, Val42, Asn44 and Leu110). Interestingly, all residues of apoALA and holoALA interacting with EGCG are found to be involved in interactions of vitamin D docked to ALA (Delavari, et al., 2015), also pointing out to the same binding site (Fig. 2B).

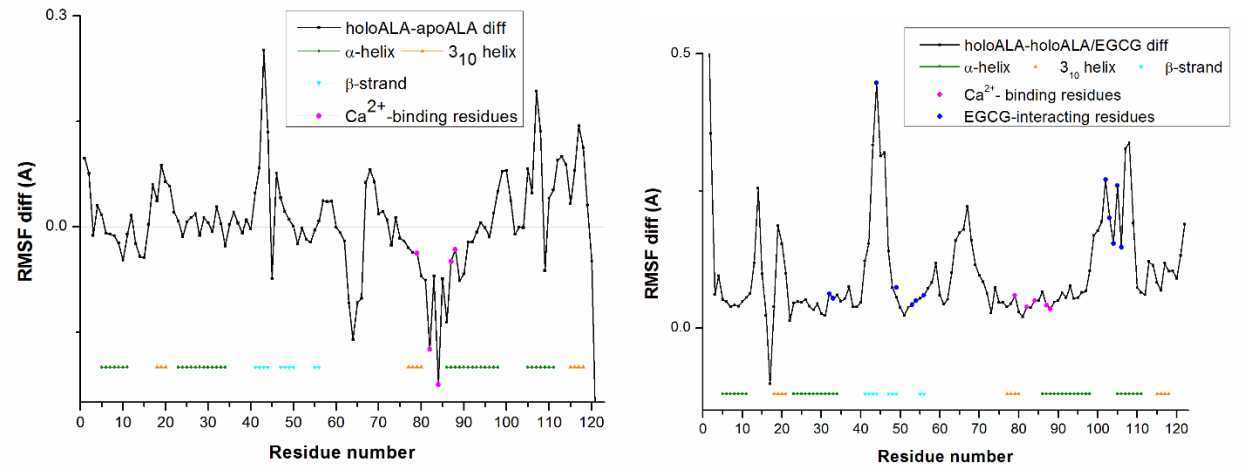

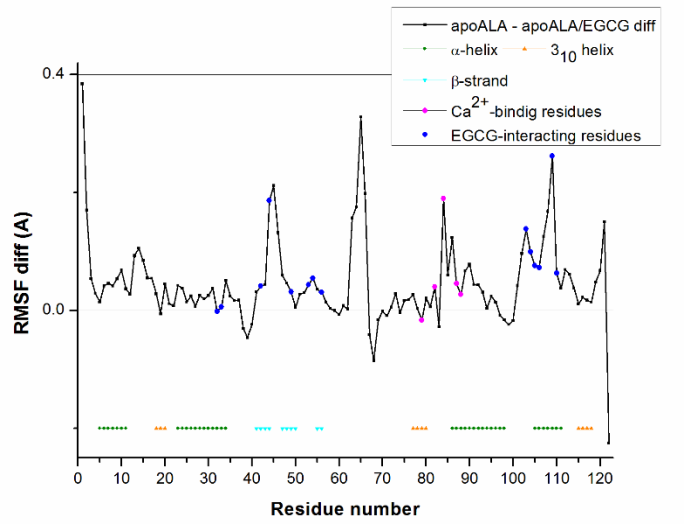

Fig 4. Molecular dynamics simulation of holoALA, holoALA-EGCG, apoALA and apoALA-EGCG. Difference of RMSF values between holoALA and apoALA (**A**), holoALA and holoALA-EGCG (**B**), and apoALA and apoALA-EGCG (**C**) with marked amino acid residues involved in Ca2+ binding, EGCG-interacting residues and regions with secondary structures.

Comparison of backbone root mean square fluctuations (RMSF) of holoALA and apo ALA (Fig. 6A and S6 demonstrate that removal of Ca^{2+} resulted in higher flexibility of Ca^{2+}-binding site region (including H3-helix, 75-96 aa), C-terminus and loop 2 (60-66 aa) with slight increase in rigidity of other parts. Obtained RMSF profiles are in accordance to B-factors obtained for crystal structures of holoALA and apoALA (Chrysina, Brew, & Acharya, 2000), showing that the absence of calcium also results in an slight increase in mobility in the Ca^{2+}-binding site and C-terminal, but a decrease in mobility of β-lobe. In addition, NMR spectroscopy demonstrated substantial increase of ALA dynamics of Ca^{2+} binding region and H3-helix in the absence of Ca^{2+} and real-time NMR experiments showed that conversion of the holoALA to apoALA involve local reorganizations of the structure in the vicinity of the Ca^{2+}-binding site (Wijesinha-Bettoni, Dobson, & Redfield, 2001). Both crystal structure (Chrysina, Brew, & Acharya, 2000) and NMR study of apoALA, were done in high concentration of NaCl and represented native apoALA. Both studies confirmed that stabilization of the native state of the apoALA by higher concentrations of monovalent cations results from the screening of repulsive negative charges, at the Ca^{2+}-binding site, rather than by specific binding to replace Ca^{2+} ions. For our MDS starting structures were solvated, with addition of Na^{+} and Cl^{-} ions (150 mM) added to counter the total

charge of the protein. All this implies that, simulation of Ca^{2+} removal from holoALA used in this study results in structure behaving as apoALA form, and that in MDS our apoALA behaves as native apoALA.

According to RMSF profiles of holoALA and holoALA-EGCG, the whole sequence of holoALA is stabilized by EGCG, with both β-lobe loops and 97-110 aa regions the most stabilized (Fig. 4B and S7). Stabilization of region 100-110 aa and β-lobe loop 1 (43-47 aa) is direct consequence of interactions of residing residues with EGCG (Fig. 4B). EGCG binding induce greater stability and compactness of holoALA according to Rg and RMSD (Fig S2~~=~~7).

RMSF profiles of apoALA and apoALA-EGCG indicate that EGCG bound to apoALA also decrease its flexibility, mostly in β-lobe loops and 97-110 aa regions (Figs. 4C and S8). However, in apoALA EGCG additionally stabilize Ca^{2+}-binding loop and especially H3 helix (84-98 aa) bearing three Ca^{2+}-binding residues, Asp84, Asp87 and Asp88. As mentioned above this is the main region destabilized when Ca^{2+} was removed from holoALA (Fig. 4A). This suggests that EGCG binding can revert stability of Ca^{2+}-binding region in native apoALA. ApoALA stabilization by EGCG can be also noticed from Rg (Figs. S8B and S8D), RMSD (Fig S9) and 2D RMSD plots (Fig. S10). Also, inside of Ca^{2+}-binding loop, EGCG binding restores longevity of Lys79-Asp82 salt bridge therefore contributing to stability of Ca^{2+}-binding region (Fig. S11). These results suggest that EGCG binding stabilize apoALA mainly by reversion of stability of Ca^{2+}-binding region.

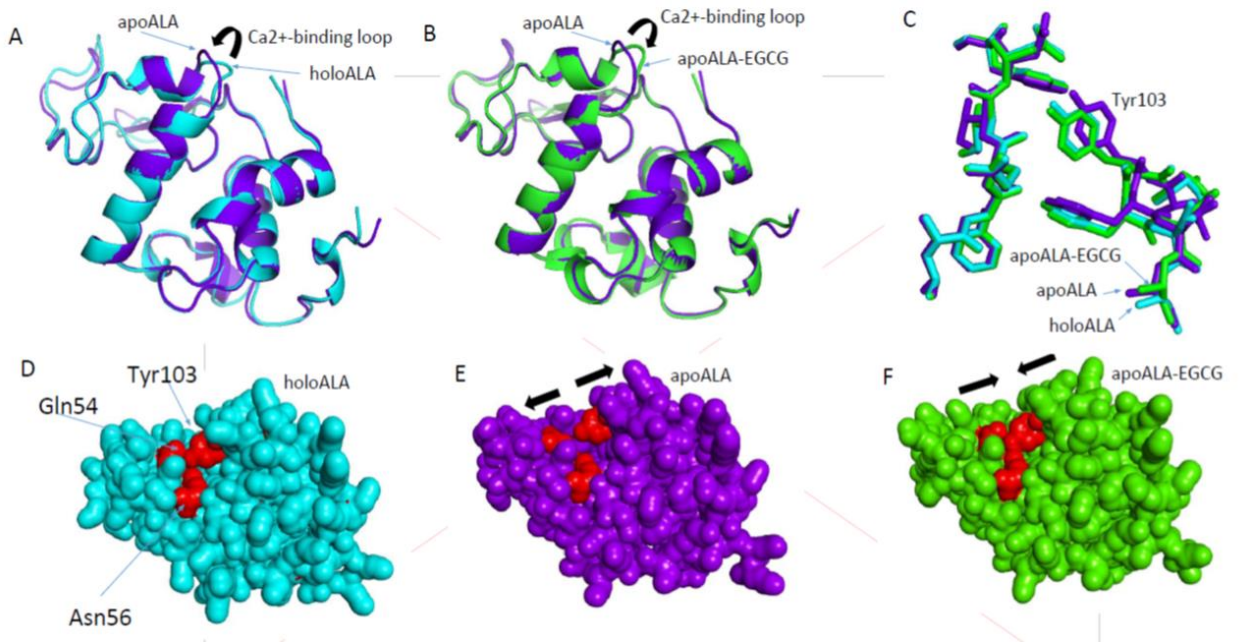

Fig 5. Overlapped conformations of holoALA and apoALA (**A**) and apoALA and apoALA-EGCG (**B**) after MDS. The black arrows direct to region the most affected by Ca2+ removal and reverted by EGCG-binding. Superpositions of residues at the entrance of the cleft of holoALA, apoALA and apoALA-EGCG showing perturbation of Tyr103 by Ca2+removal and its restored position by EGCG binding (**C**). Molecular surfaces of holoALA (**D**), apoALA (**E**) and apoALA-EGCG (**F**) showing the entrance of the cleft after MDS. The perturbation of Tyr103 in apoALA results in a slight opening of the cleft, while EGCG binding restore cleft tightness. HoloALA structure is represented in cyan, apoALA in violet and apoALA-EGCG in green. All structures are based on averaged conformations of the main cluster for holoALA, apoALA and apoALA-EGCG after MDS. ApoALA structure was obtained by Ca2+ removal from crystal structure of holoALA (PDB ID 1F6S).

Reversion of apoALA stability by EGCG can be observed also by inspection of several details in resultant structural changes. During MDS, in apoALA Ca^{2+} removal induced noticeable bending of Ca^{2+}-binding loop (Fig. 5A) and EGCG reverts Ca^{2+}-binding loop conformation similar to holoALA (Fig. 5B). Indeed, average mutual distances between Ca^{2+}- binding residues are increased in apoALA, due to absence of Ca^{2+} to stick them together. The presence of EGCG mostly shorten back these distances resulting in more stable Ca^{2+}-binding region (Figs. S12 and S13). According to crystal structures of holoALA and apoALA, Ca^{2+} removal has only minor

effects on ALA structure, with the largest structural change in the cleft propagated from the Ca^{2+}-binding loop. There, Tyr103 changed its orientation and water mediated interactions with Gln54 and Asn56 replace direct hydrogen bonds, and consequence of this is separation of α and β subdomains, resulting in a more open cleft in the apoALA (Chrysina, Brew, & Acharya, 2000). Indeed, during simulation time, at the entrance of the cleft the effect of Ca^{2+} removal can be observed in perturbation of Tyr103, and EGCG binding induce reversion of Tyr103 to orientation similar to holoALA (Fig. 5C). Also, EGCG binding reverts back short Tyr103-Gln54 and Tyr103-Asn56 distances, therefore allowing recovery of direct hydrogen bonds (Fig. S14). Moreover, after MDS, perturbation of Tyr103 in apoALA also resulted in opening the cleft due to slight separation of α and β lobes (Figs. 5D and 5E). EGCG binding to apoALA jointed back α and β subdomains by reversion of Tyr103 orientation (Fig. 5F). Therefore, EGCG binding to apoALA mostly reverts Ca^{2+}-binding loop conformation and its stability during the time, which is propagated to the cleft, resulting in re-joining of subdomains and cleft closing by the same mechanism.

It was proposed that in apoALA, at low ionic strength, increased charge repulsion will further expand the Ca^{2+}-binding region leading to further separation of the subdomains and sufficient disruption of interactions in the hydrophobic box to result in a loss of net stability in the native structure (Chrysina, Brew, & Acharya, 2000). It seems that, at lower ionic strength, EGCG would also at least partially stabilize apoALA by postponing expansion of Ca^{2+}-binding loop and consequent further separation of lobes, as well as by impeding disruption of interactions in the hydrophobic box, as EGCG actually binds to hydrophobic box residues (Fig. 2B). As native apoALA conformation is regarded as initial step in the transition to the molten globule (Chrysina, Brew, & Acharya, 2000), EGCG binding is probably able to retard transition of native apoALA to molten globule (MG), e.g. to increase the stability of native apoALA relative to MG state in conditions favouring MG.

4. Conclusions

Investigation carried out in this study, by the experimental and computational approach, gave insight into interactions between apoALA and EGCG. Fluorescence quenching revealed that the main green tea catechin, EGCG, binds to both holoALA and apoALA, at neutral (pH 7.2) and

acidic conditions (pH 2.5 and pH 1.2), at low (6 ºC) and physiological temperature (37 ºC). EGCG binds to holoALA and apoALA at all tested conditions with Ka of similar magnitude, but has lower affinity at conditions where ALA has less ordered structure. CD spectroscopy demonstrated that EGCG binds to apoALA regardless is it in its native or molten globule state, thereby inducing only slight change in secondary and tertiary structure. At neutral conditions, EGCG binding resulted in thermal stabilization of apoALA, as reflected in EGCG-depending increased Tm, and this stabilization is more pronounced than for holo form.

The docking analysis showed that EGCG binds to apoALA at the same site as to holo form, at the entrance of cleft between α and β lobes, and molecular dynamic simulation (MDS) demonstrated that it remained bound at the same site during the time. MDS revealed that Ca^{2+} removal results in decreased conformational stability of ALA, where disturbed Ca^{2+}-binding region resulted in slight opening the cleft due to separation of α and β lobes. EGCG binding to apoALA increase its stability by reverting stability of Ca^{2+}-binding region, which is inversely transmitted to cleft, with re-joining of subdomains and cleft closing outcome. Therefore, experimentally observed increased EGCG-induced thermal stability of apoALA is based on increased apoALA conformational rigidity due to its binding. The mitigating of apoALA instability by EGCG implies that EGCG binding could stabilize apoALA at lower ionic strength and postpone transformation of native apoALA to molten globule under conditions favouring its formation.

The results of this study together demonstrate that, similarly to holo form, ALA in its apo form can be also used as vehicle for delivery of EGCG. Moreover, the substantial binding of EGCG to ALA at acidic conditions and at 37 ^{o}C suggests that, after ingestion of tea with milk, or food fortified with EGCG encapsulated in holoALA-based carriers, in gastric compartment EGCG would be still bound to ALA, in spite that it is in apo form.

Acknowledgment

This research was carried out with the support from the Ministry of Education and Science of the Republic of Serbia, GA No. OI172024, and the European Commission, under the Horizon2020, FoodEnTwin project, GA No.810752. The EC does not share responsibility for the content of the article

References

Al-Hanish, A., Stanic-Vucinic, D., Mihailovic, J., Prodic, I., Minic, S., Stojadinovic, M., Radibratovic, M., Milcic, M., & Cirkovic Velickovic, T. (2016). Noncovalent interactions of bovine α-lactalbumin with green tea polyphenol, epigalocatechin-3-gallate. *Food Hydrocolloids, 61*, 241-250.

Amirdivani, S., & Baba, A. S. H. (2015). Green tea yogurt: major phenolic compounds and microbial growth. *Journal of Food Science and Technology-Mysore, 52*(7), 4652-4660.

Anandakrishnan, R., Aguilar, B., & Onufriev, A. V. (2012). H++ 3.0: automating pK prediction and the preparation of biomolecular structures for atomistic molecular modeling and simulations. *Nucleic Acids Research, 40*(W1), W537-W541.

Barbana, C., Perez, M. D., Sanchez, L., Dalgalarrondo, M., Chobert, J. M., & Haertle, T. (2006). Interaction of bovine alpha-lactalbumin with fatty acids as determined by partition equilibrium and fluorescence spectroscopy. *International Dairy Journal, 16*(1), 18-25.

Bi, S., Ding, L., Tian, Y., Song, D., Zhou, X., Liu, X., & Zhang, H. (2004). Investigation of the interaction between flavonoids and human serum albumin. *Journal of Molecular Structure, 703*(1-3), 37-45.

Chakraborty, S., Ittah, V., Bai, P., Luo, L., Haas, E., & Peng, Z. Y. (2001). Structure and dynamics of the alpha-lactalbumin molten globule: Fluorescence studies using proteins containing a single tryptophan residue. *Biochemistry, 40*(24), 7228-7238.

Chaudhuri, A., & Chattopadhyay, A. (2014). Lipid binding specificity of bovine alpha-lactalbumin: a multidimensional approach. *Biochim Biophys Acta, 1838*(8), 2078-2086.

Chrysina, E. D., Brew, K., & Acharya, K. R. (2000). Crystal structures of apo- and holo-bovine alpha-lactalbumin at 2. 2-A resolution reveal an effect of calcium on inter-lobe interactions. *J Biol Chem, 275*(47), 37021-37029.

Delavari, B., Saboury, A. A., Atri, M. S., Ghasemi, A., Bigdeli, B., Khammari, A., Maghami, P., Moosavi-Movahedi, A. A., Haertle, T., & Goliaei, B. (2015). Alpha-lactalbumin: A new carrier for vitamin D-3 food enrichment. *Food Hydrocolloids, 45*, 124-131.

Ferruzzi, M. G. (2010). The influence of beverage composition on delivery of phenolic compounds from coffee and tea. *Physiol Behav, 100*(1), 33-41.

Hemar, Y., Gerbeaud, M., Oliver, C. M., & Augustin, M. A. (2011). Investigation into the interaction between resveratrol and whey proteins using fluorescence spectroscopy. *International Journal of Food Science and Technology, 46*(10), 2137-2144.

Humphrey, W., Dalke, A., & Schulten, K. (1996). VMD: Visual molecular dynamics. *Journal of Molecular Graphics, 14*(1), 33-38.

Layman, D. K., Lonnerdal, B., & Fernstrom, J. D. (2018). Applications for alpha-lactalbumin in human nutrition. *Nutrition Reviews, 76*(6), 444-460.

Mackerell, A. D., Feig, M., & Brooks, C. L. (2004). Extending the treatment of backbone energetics in protein force fields: Limitations of gas-phase quantum mechanics in reproducing protein conformational distributions in molecular dynamics simulations. *Journal of Computational Chemistry, 25*(11), 1400-1415.

Malinovskii, V. A., Tian, J., Grobler, J. A., & Brew, K. (1996). Functional site in alpha-lactalbumin encompasses a region corresponding to a subsite in lysozyme and parts of two adjacent flexible substructures. *Biochemistry, 35*(30), 9710-9715.

Mohammadi, F., & Moeeni, M. (2015a). Analysis of binding interaction of genistein and kaempferol with bovine alpha-lactalbumin. *Journal of Functional Foods, 12*, 458-467.
Mohammadi, F., & Moeeni, M. (2015b). Study on the interactions of trans-resveratrol and curcumin with bovine alpha-lactalbumin by spectroscopic analysis and molecular docking. *Mater Sci Eng C Mater Biol Appl, 50*, 358-366.
Mok, K. H., Pettersson, J., Orrenius, S., & Svanborg, C. (2007). HAMLET, protein folding, and tumor cell death. *Biochemical and Biophysical Research Communications, 354*(1), 1-7.
Najgebauer-Lejko, D., Sady, M., Grega, T., & Walczycka, M. (2011). The impact of tea supplementation on microflora, pH and antioxidant capacity of yoghurt. *International Dairy Journal, 21*(8), 568-574.
Nikoo, M., Regenstein, J. M., & Gavlighi, H. A. (2018). Antioxidant and Antimicrobial Activities of (-)-Epigallocatechin-3-gallate (EGCG) and its Potential to Preserve the Quality and Safety of Foods. *Comprehensive Reviews in Food Science and Food Safety, 17*(3), 732-753.
Permyakov, E. A., & Berliner, L. J. (2000). alpha-Lactalbumin: structure and function. *FEBS Lett, 473*(3), 269-274.
Permyakov, E. A., Grishchenko, V. M., Kalinichenko, L. P., Orlov, N. Y., Kuwajima, K., & Sugai, S. (1991). Calcium-regulated interactions of human alpha-lactalbumin with bee venom melittin. *Biophys Chem, 39*(2), 111-117.
Permyakov, E. A., Permyakov, S. E., Deikus, G. Y., Morozova-Roche, L. A., Grishchenko, V. M., Kalinichenko, L. P., & Uversky, V. N. (2003). Ultraviolet illumination-induced reduction of alpha-lactalbumin disulfide bridges. *Proteins-Structure Function and Genetics, 51*(4), 498-503.
Perusko, M., Al-Hanish, A., Mihailovic, J., Minic, S., Trifunovic, S., Prodic, I., & Cirkovic Velickovic, T. (2017). Antioxidative capacity and binding affinity of the complex of green tea catechin and beta-lactoglobulin glycated by the Maillard reaction. *Food Chem, 232*, 744-752.
Pettersen, E. F., Goddard, T. D., Huang, C. C., Couch, G. S., Greenblatt, D. M., Meng, E. C., & Ferrin, T. E. (2004). UCSF Chimera—A visualization system for exploratory research and analysis. *Journal of Computational Chemistry, 25*(13), 1605-1612.
Phillips, J. C., Braun, R., Wang, W., Gumbart, J., Tajkhorshid, E., Villa, E., Chipot, C., Skeel, R. D., Kalé, L., & Schulten, K. (2005). Scalable molecular dynamics with NAMD. *Journal of Computational Chemistry, 26*(16), 1781-1802.
Popov, A. V., Vorobjev, Y. N., & Zharkov, D. O. (2012). MDTRA: A molecular dynamics trajectory analyzer with a graphical user interface. *Journal of Computational Chemistry, 34*(4), 319-325.
Prigent, S. V. E., Voragen, A. G. J., van Koningsveld, G. A., Baron, A., Renard, C. M. G. C., & Gruppen, H. (2009). Interactions between globular proteins and procyanidins of different degrees of polymerization. *Journal of Dairy Science, 92*(12), 5843-5853.
Rashidinejad, A., Birch, E. J., & Everett, D. W. (2016). The behaviour of green tea catechins in a full-fat milk system under conditions mimicking the cheesemaking process. *International Journal of Food Sciences and Nutrition, 67*(6), 624-631.
Rashidinejad, A., Birch, E. J., Sun-Waterhouse, D., & Everett, D. W. (2014). Delivery of green tea catechin and epigallocatechin gallate in liposomes incorporated into low-fat hard cheese. *Food Chemistry, 156*, 176-183.

Shi, M., Shi, Y. L., Li, X. M., Yang, R., Cai, Z. Y., Li, Q. S., Ma, S. C., Ye, J. H., Lu, J. L., Liang, Y. R., & Zheng, X. Q. (2018). Food-Grade Encapsulation Systems for (-)-Epigallocatechin Gallate. *Molecules, 23*(2).

Stanciuc, N., Turturica, M., Oancea, A. M., Barbu, V., Ionita, E., Aprodu, I., & Rapeanu, G. (2017). Microencapsulation of Anthocyanins from Grape Skins by Whey Protein Isolates and Different Polymers. *Food and Bioprocess Technology, 10*(9), 1715-1726.

Sugai, S., & Ikeguchi, M. (1994). Conformational comparison between alpha-lactalbumin and lysozyme. *Adv Biophys, 30*, 37-84.

Trott, O., & Olson, A. J. (2009). AutoDock Vina: Improving the speed and accuracy of docking with a new scoring function, efficient optimization, and multithreading. *Journal of Computational Chemistry, 31*(2), 455-461.

Veprintsev, D. B., Permyakov, S. E., Permyakov, E. A., Rogov, V. V., Cawthern, K. M., & Berliner, L. J. (1997). Cooperative thermal transitions of bovine and human apo-alpha-lactalbumins: evidence for a new intermediate state. *FEBS Lett, 412*(3), 625-628.

Vesic, J., Stambolic, I., Apostolovic, D., Milcic, M., Stanic-Vucinic, D., & Cirkovic Velickovic, T. (2015). Complexes of green tea polyphenol, epigalocatechin-3-gallate, and 2S albumins of peanut. *Food Chem, 185*, 309-317.

Wang, X. Y., Zhang, J., Lei, F., Liang, C. X., Yuan, F., & Gao, Y. X. (2014). Covalent complexation and functional evaluation of (-)-epigallocatechin gallate and alpha-lactalbumin. *Food Chemistry, 150*, 341-347.

Wijesinha-Bettoni, R., Dobson, C. M., & Redfield, C. (2001). Comparison of the structural and dynamical properties of holo and apo bovine alpha-lactalbumin by NMR spectroscopy. *J Mol Biol, 307*(3), 885-898.

Zhang, H., Yu, D. D., Sun, J., Guo, H. Y., Ding, Q. B., Liu, R. H., & Ren, F. Z. (2014). Interaction of milk whey protein with common phenolic acids. *Journal of Molecular Structure, 1058*, 228-233.